ELSEVIER

Biophysical Chemistry 99 (2002) 117–127

Biophysical Chemistry

www.elsevier.com/locate/bpc

# Differential effects of cholesterol on acyl chain order in erythrocyte membranes as a function of depth from the surface. An electron paramagnetic resonance (EPR) spin label study

M.B. Cassera[a,1], A.M. Silber[a,2], A.M. Gennaro[a,b,*]

[a]*Facultad de Bioquímica y Ciencias Biológicas, Universidad Nacional de Litoral, Paraje El Pozo S/N, 3000 Santa Fe, Argentina*
[b]*INTEC (CONICET-UNL), Güemes 3450, 3000 Santa Fe, Argentina*

Received 24 January 2002; received in revised form 7 May 2002; accepted 7 May 2002

**Abstract**

The purpose of this work is to analyze the effects of cholesterol modulation on acyl chain ordering in the membrane of human erythrocytes as a function of depth from the surface. Partial cholesterol depletion was achieved by incubation of erythrocytes with liposomes containing saturated phospholipids, or with methyl-β-cyclodextrin (MβCD). Cholesterol enrichment was achieved by incubation with liposomes formed by phospholipids/cholesterol, or with the complex MβCD/cholesterol. Acyl chain order was studied with electron paramagnetic resonance spectroscopy (EPR) using spin labels that sense the lipid bilayer at different depths. It is shown that the increase in cholesterol stiffens acyl chains but decreases the interaction among lipid headgroups, while cholesterol depletion causes the opposite behavior. It is likely that the observed cholesterol effects are related to those stabilizing the cholesterol-rich detergent-insoluble membrane domains (rafts), recently shown to exist in erythrocytes.


*Keywords:* Cholesterol modulation; Erythrocyte membrane fluidity; EPR order parameter; Cyclodextrins; Liposomes; Rafts

*Corresponding author. Tel.: +54-342-457-5213; fax: +54-342-455-0944.
*E-mail address:* agennaro@intec.unl.edu.ar (A.M. Gennaro).
[1] Present address: Departamento de Parasitologia, Instituto de Ciências Biomédicas, Universidade de São Paulo, Av. Lineu Prestes 1374, CEP: 05508-900, São Paulo, SP Brasil.
[2] Present address: Laboratório de Bioquímica de Parasitas, Departamento de Bioquímica, Instituto de Química, Universidade de São Paulo, Av. Lineu Prestes 748, Bloco 10 I, CEP: 05508-900, São Paulo, SP Brasil.

0301-4622/02/$ - see front matter 
PII: S0301-4622(02)00139-4

## 1. Introduction

In mature human erythrocytes, nucleus and organelles are missing, and they consist essentially of a plasmatic membrane enclosing a hemoglobin solution. Half of the membrane mass is represented by protein and the other half by lipid, mainly phospholipids and cholesterol, with a molar relation cholesterol to phospholipid of about 0.9 [1].

Cholesterol is important as a regulator of the physical state of lipid bilayers, and is necessary for the functional activity of several membrane proteins [2]. A specific physical characteristic of the cholesterol molecule is its almost planar steroid ring, a structure with a rigid conformation. It is reasonable to imagine that this feature could impose motional and/or positional restrictions to neighbor lipid molecules in the membrane structure. In fact, a lot of experimental evidence has been accumulated showing that membrane 'fluidity' is reduced when cholesterol levels are increased (see for instance van der Meer [3] and references therein). However, the term 'fluidity' generalizes many aspects of molecular degrees of freedom, not all of which are directly related to each other or to the same biological phenomenon. Thus, it would be desirable to obtain information about the way in which specific degrees of freedom are affected by cholesterol modulation.

The effects of changing cholesterol concentrations in different phases of model membranes composed of pure lipids are rather well understood [4,5]. However, when cholesterol is added to lipid mixtures, the phenomenon of lateral segregation precludes a simple prediction of the effects of cholesterol variation. In a natural membrane, the presence of proteins and the asymmetry of the bilayer pose additional difficulties to establish general rules. Recently, it was found that 'rafts' enriched in cholesterol, sphingolipids and glycosylphosphatidylinositol anchored proteins, are involved in several significant cell functions and can be isolated from certain cell membranes in the form of patches resistant to cold non-ionic detergent extraction [6–8]. Structures similar to these rafts have been observed in model systems composed by the appropriate lipids [9], and recently the isolation of rafts from erythrocyte membranes [10,11] has been reported. Evidence has been accumulated suggesting that the physical state of raft lipids is the 'liquid ordered' state [4,12], in which a high lateral mobility coexists with a high degree of acyl chain order induced by the presence of cholesterol. Besides, cholesterol seems to be critical in maintaining erythrocyte raft integrity [13]. Thus, detailed knowledge about modifications of membrane physical properties by cholesterol modulation in intact erythrocytes could help to understand some of the intriguing properties of these structures. This information could be obtained with liposoluble labels that sense the hydrophobic core of membranes at different depths [14,15].

The existence of only a plasmatic membrane renders the erythrocyte as one of the simplest systems for the study of membranes in whole cells. Several studies have been performed varying the cholesterol content in erythrocyte membranes [1,16–22]. Many of these papers employed fluorescence techniques to evaluate changes on the physical characteristics of the membrane [16,20,22]. In those cases, a previous step of hemolysis is required to eliminate the interference of hemoglobin. This step submits the membrane to osmotic stresses, which could leave it in a different physical situation as compared to that of a living erythrocyte. In other cases, the techniques used to quantify cholesterol require the previous incorporation of radiolabeled cholesterol, involving additional treatments, which in turn could affect the physical state of the membrane [17,18,21].

In the present work, cholesterol content in the membrane of whole fresh erythrocytes was modified, and the changes in acyl chain ordering were quantified as a function of depth from the surface. Two approaches were applied to modify the cholesterol content of intact cells: a slow treatment involving liposomes of controlled composition; or a rapid procedure which uses methyl-beta cyclodextrin (MβCD), or the complex MβCD/cholesterol. Acyl chain ordering at different depths inside the lipid bilayer was quantified using liposoluble spin labels and EPR spectroscopy.

## 2. Experimental procedures

### 2.1. Chemicals

Spin labels, cholesterol (crystalline, +99% purity), Triton X-100, phospholipids and methyl-β-cyclodextrin (MβCD) were purchased from Sigma Chemical Co. (St. Louis, USA). Solvents, inorganic salts and all other chemicals were of the highest quality commercially available. Analytical grade enzymatic reagents for cholesterol determination were from Merck (Germany) and Seppim-Elitech (Sees, France). The liposoluble *n*-doxyl stearic acid positional isomers (*n*-SASL, $n=5$, 12 and 16) were used as spin labels.

### 2.2. Separation of red blood cells

Fresh human blood (5–10 ml) was collected from healthy donors among laboratory personnel. Heparin solution was used as anticoagulant. Erythrocytes were separated from plasma and buffy coat by centrifugation at $2000\times g$ for 5 min, washed three times in isotonic phosphate buffered saline (PBS, 120 mM NaCl, 30 mM $Na_2HPO_4$, 6 mM $KH_2PO_4$, 11 mM glucose, pH 7.4) and immediately processed as follows.

### 2.3. Manipulation of cholesterol content in red blood cell membranes using liposomes

Liposomes were prepared by sonication, according to Cooper et al. [1] and Thompson and Axelrod [20], with two saturated phospholipids of different acyl chain lengths: dipalmitoyl phosphatidylcholine (DPPC, 16 carbons), or dimyristoyl phosphatidylcholine (DMPC, 14 carbons). Liposomes containing phospholipids were used for cholesterol depletion, and mixtures of phospholipid and cholesterol for cholesterol enrichment. Lipids were dispersed in PBS or in Hank's isotonic saline solution (5 mM KCl, 0.2 mM $Na_2HPO_4$, 0.4 mM $KH_2PO_4$, 4 mM $NaHCO_3$, 12 mM $CaCl_2$, 1.2 mM $MgCl_2$, 0.6 mM $MgSO_4$, 137 mM NaCl, 5 mM $C_6H_{12}O_6$, pH 7.4). Antibiotics were supplied to the incubation medium to prevent growth of bacteria.

#### 2.3.1. Cholesterol depletion

Twenty-five milligrams of phospholipids (DMPC or DPPC) were weighted in a PVC tube, followed by the addition of 2.5 ml PBS. The suspension was sonicated by pulses with a titanium probe (Sonic and Materials, CT, USA) in an ice bath, until a opalescent solution was obtained (after approx. 1 h). A centrifugation for 10 min at $2700\times g$ was performed to sediment titanium impurities and non dissolved lipids. Then, 400 μl of packed cells were added to the supernatant (final volume concentration approximately 15%). The incubations were performed in the presence of ampicillin and tetracycline. The red blood cells/liposome suspension was incubated for 30 h at 37 °C with vigorous shaking. Cells were separated by centrifugation and washed four times with several volumes of isotonic PBS.

#### 2.3.2. Cholesterol enrichment

Forty milligrams cholesterol and 20 mg phospholipid were added to 5 ml of Hank's solution and the mixture was submitted to pulsed probe sonication in an ice bath, until a milky homogenous solution was obtained (close to 1 h). Then, 2 ml of heat inactivated serum were added. The suspension was centrifuged at $2700\times g$ for 15 min at 7 °C and the precipitate discarded. Seven hundred μl of packed cells resuspended in 6.3 ml of Hank's solution were added to the supernatant (final volume concentration approx. 5%). The incubations were performed in the presence of ampicillin and tetracycline for 30 h at 37 °C with vigorous shaking. Following incubation, cells were collected by centrifugation and washed four times in several volumes of isotonic PBS as previously described.

In both cases, control cells were processed exactly the same way, but in an incubation medium lacking liposomes. Aliquots from control and treated samples were used for cholesterol enzymatic quantification, microscopy and EPR experiments.

### 2.4. Manipulation of cholesterol content in red blood cell membranes with methyl-β-cyclodextrin

Methyl-β-cyclodextrin (MβCD) is an efficient agent for removing cholesterol from culture and

suspended cells [21,23,24]. The complex MβCD/cholesterol has also been used to produce cholesterol enrichment [24–26]. It has been proven that MβCD does not incorporate into treated membranes [21].

A stock solution of 20 mM MβCD in PBS was prepared and kept at 4 °C in the dark. Cholesterol (40 mg) was dissolved in 1 ml chloroform/methanol (1:1). The solvent was evaporated under a nitrogen stream to obtain a dry film. MβCD stock solution (30 ml) was added, vortexed and sonicated for a few minutes in a water bath. The mixture was agitated overnight at 37 °C, and then it was centrifuged at 2700×*g* for 10 min. The supernatant was kept in a dark flask. Previous to use, it was filtered with a 0.45 μm syringe filter. The resultant cholesterol concentration was 0.84 mg/ml, equivalent to 32 mg cholesterol/g MβCD.

Three millimolar MβCD (for depletion) or MβCD/cholesterol (for enrichment) in PBS were incubated with 5 or 10% erythrocyte volume concentration (hematocrit), in PVC tubes at 37 °C, with occasional mixing. Lower hematocrits were not used due to the significant degree of hemolysis observed in these cases. Control erythrocytes were incubated in PBS at the same concentration. After 30 min of incubation, the tubes were centrifuged for 2 min at 1500×*g*. The supernatants were preserved to determine the degree of hemolysis, and the pelleted erythrocytes were washed twice with PBS.

### 2.5. Determination of membrane cholesterol concentration

Cholesterol content of erythrocyte membranes was determined after lipid extraction [27] using a modified cholesterol-oxidase method (see as instance [28]). Briefly, 100 μl of packed erythrocytes was lysed in 120 μl distilled water. After 15 min incubation at room temperature, 1.35 ml of 2-propanol was added with vortexing. After 1 h of incubation, 0.75 ml of chloroform were added while vortexing, and after 1 h incubation, the suspension was centrifuged for 10 min at 2700×*g* for 10 min, and the clear organic layer was separated. The organic solvent was evaporated, and the lipid extract was reconstituted in 150 μl ethanol [29]. Of this solution, 20 μl were incubated with 2 ml of the enzymatic solution, containing 0.5% v/v Triton X-100. The absorbance was read at 500 nm in a Perkin-Elmer Lambda 20 spectrometer, against the enzymatic solution as blank. Each experiment was performed in triplicate.

### 2.6. EPR experiments and data analysis

The liposoluble n-doxyl-stearic acid spin labels (n-SASL) bear a nitroxide moiety at the position $n=5$, 12 or 16 of a stearic acid chain. They were incorporated to the erythrocyte membranes to a final spin label/membrane lipid molar ratio less than 1%, in order to avoid line broadening effects in the EPR spectra. For labeling, the appropriate amount of the chosen spin label ethanol solution (usually 1.3 μl, which evaporated almost instantaneously) was poured into a PVC tube. PBS buffer (675 μl) was added and gently agitated, followed by 75 μl of packed erythrocytes. The solution was homogenized by several steps of suction and expulsion with the micropipette tip. After 30 min incubation at room temperature, tubes were centrifuged at 1500×*g* and the supernatant was discarded. Aliquots of the erythrocyte pellet (usually 20 μl) were transferred into glass capillaries (1 mm i.d.), flame sealed and put into 4 mm quartz tubes. This procedure was used both for control and pre-treated samples. The EPR spectra were recorded at (25±1) °C and 9.8 GHz (X Band) in a ER-200 spectrometer (Bruker Analytische Messtechnik GMbH, Karlsruhe, Germany). Field modulation frequency was 100 kHz, and modulation amplitude was well below 30% of the minor linewidths, in order to avoid spectral shape distortions.

From the EPR spectra of 5-, 12- and 16-SASL (Fig. 1), which sense the bilayer at different depths, an apparent order parameter $S_{app}$ [30] can be evaluated as:

$$S_{app}=(1/k_0)(A_{//}-A_{\perp})/\left[A^c_{zz}-\frac{1}{2}(A^c_{xx}+A^c_{yy})\right]$$

where

$$A_{//}=A_{max};\ A_{\perp}=A_{min}+1.4(1-S_0)$$

with

$$A_{\max}=\frac{1}{2}(B_4-B_1);\ A_{\min}=\frac{1}{2}(B_3-B_2);$$

$$S_0=(A_{\max}-A_{\min})/\left[A^{c}_{zz}-\frac{1}{2}(A^{c}_{xx}+A^{c}_{yy})\right],$$

$$A^{c}_{0}=\frac{1}{3}(A^{c}_{zz}+A^{c}_{xx}+A^{c}_{yy}),$$

$$A_0=\frac{1}{3}(A_{//}+2A_{\perp}),\ \text{and}\ k_0=A_0/A^{c}_{0}$$

$B_1$ to $B_4$ (pointed out with arrows in Fig. 1) are magnetic field values for spectrum structures related to the hyperfine interaction between the radical unpaired electron and the $^{14}N$ nucleus. The parameters $A^{c}_{zz}=32.9$ gauss, $A^{c}_{xx}=5.9$ gauss and $A^{c}_{yy}=5.4$ gauss are the single crystal values of the $^{14}N$ hyperfine coupling tensor [30].

The apparent order parameter is related to the angular amplitude of motion of the labeled segment, and its values lie in the range $0<S_{app}<1$. Values of $S_{app}$ near 1 would be obtained for a label into a structure with fully aligned all-trans acyl chains, while $S_{app}$ close to zero indicates unrestricted isotropic movements of the spin label at the corresponding position. Thus, an increase in $S_{app}$ implies a straightening of the acyl chains (i.e. increased order) at the level where the labeled moiety is inserted and vice versa. These features are governed by trans-gauche (t-g) isomerizations, which confer flexibility to the acyl chains [30]. The plot of $S_{app}$ as a function of the position of the label, sometimes called 'flexibility gradient', represents a depth profiling showing how the order parameter decreases towards the membrane hydrophobic core. The comparison of flexibility gradients is useful to compare different degrees of t-g isomerization, as well as to locate the depth at which changes occur among different samples of similar composition [14].

### 2.7. Microscopic analysis

Immediately after each treatment, 'fresh drop' images of control and treated cells were obtained. Small aliquots of diluted control and treated cells

Table 1
Apparent order parameters $S_{app}$ obtained from EPR spectra of the spin labels 5-, 12- and 16-SASL in control, cholesterol depleted and cholesterol enriched erythrocytes

| Treatment | %Chol | 5-SASL | | | 12-SASL | | | 16-SASL | | |
|---|---|---|---|---|---|---|---|---|---|---|
| | | $S^{control}_{app}$ | $S^{treated}_{app}$ | l.s.[i] | $S^{control}_{app}$ | $S^{treated}_{app}$ | l.s.[i] | $S^{control}_{app}$ | $S^{treated}_{app}$ | l.s.[i] |
| | 30 (3)[a] | 0.668 (2) | 0.683 (1) | $P<0.001$ | 0.541 (2) | 0.514 (7) | $P<0.01$ | 0.227 (1) | 0.200 (1) | $P<0.001$ |
| Cholesterol | 67 (7)[b] | 0.686 (4) | 0.689 (3) | n.s. | 0.536 (6) | 0.520 (4) | $P<0.02$ | 0.225 (3) | 0.217 (2) | $P<0.02$ |
| depletion | 33 (3)[c] | 0.698 (3) | 0.692 (2) | n.s. | 0.553 (10) | 0.527 (5) | $P<0.02$ | 0.253 (5) | 0.219 (5) | $P<0.01$ |
| | 60 (6)[d] | 0.685 (4) | 0.685 (6) | n.s. | 0.567 (3) | 0.559 (18) | n.s. | 0.245 (2) | 0.225 (1) | $P<0.001$ |
| | 170 (15)[e] | 0.683 (7) | 0.660 (7) | $P<0.02$ | 0.528 (7) | 0.563 (8) | $P<0.01$ | 0.232 (2) | 0.249 (2) | $P<0.001$ |
| Cholesterol | 190 (20)[f] | 0.686 (4) | 0.667 (3) | $P<0.01$ | 0.536 (6) | 0.566 (4) | $P<0.01$ | 0.225 (3) | 0.247 (2) | $P<0.001$ |
| enrichment | 125 (12)[h] | 0.680 (5) | 0.672 (4) | n.s. | 0.553 (8) | 0.548 (7) | n.s. | 0.231 (7) | 0.247 (2) | $P<0.02$ |
| | 170 (15)[g] | 0.678 (2) | 0.665 (4) | $P<0.01$ | 0.553 (4) | 0.569 (4) | $P<0.01$ | 0.241 (8) | 0.253 (4) | n.s. |

%Chol indicates the final cholesterol content of treated cells, where 100% is the cholesterol content of the corresponding control cells. Standard deviation uncertainties in the last digits of the quoted values are indicated in parentheses. Not significant: n.s.

[a] DMPC liposomes.
[b] DPPC liposomes.
[c] MβCD 3 mM, erythrocyte concentration 5% (v/v).
[d] MβCD 3 mM, erythrocyte concentration 10% (v/v).
[e] DMPC/cholesterol liposomes.
[f] DPPC/cholesterol liposomes.
[g] MβCD/cholesterol 3 mM, erythrocyte concentration 5% (v/v).
[h] MβCD/cholesterol 3 mM, erythrocyte concentration 10% (v/v).
[i] Level of significance for the hypothesis of different $S_{app}$ values between controls and treated samples (two-tailed Student's *t*-test, $n=3$).

were deposited on optical slides (previously coated with albumin solution in order to avoid the 'glass effect'), then covered with a glass coverslip and analyzed at 400× magnification (Axiolab, Carl Zeiss, Germany). Images were captured with a digital-video camera (SSC-DC50A, Sony, Japan).

In some cases, washed cells were fixed with glutaraldehyde and photographed at 1000× magnification. Also, scanning electron microscope photographs were taken for some of these fixed samples. However, comparison of fresh and fixed cell images showed shape alterations attributable to the fixation procedure. Due to this fact, and despite their poorer resolution, optical microscope images of fresh cells were chosen to better characterize shape changes.

## 3. Results

### 3.1. Changes in membrane cholesterol content

Important alterations of membrane cholesterol concentration were produced by the different treatments described previously. Initial cholesterol concentrations in untreated erythrocytes were approximately 1–1.2 mg/ml packed cells. After the treatments, final cholesterol concentrations varying between 30 and 190% relative to untreated samples were obtained (see Table 1). It is remarkable that cholesterol depletion using MβCD seems to be an abrupt process, as cells incubated only for 10 min showed essentially the same cholesterol values as those incubated 30 min. A detailed study of the time evolution of the depletion process is in progress.

### 3.2. EPR results

Fig. 1 shows typical EPR spectra of liposome treated erythrocytes: control (central spectrum of each group), cholesterol-depleted (upper spectrum) and cholesterol-enriched samples (lower spectrum), for each of the three spin labels. Arrows point out the features of the spectra whose field positions are used to calculate the order parameter $S_{app}$. Slight displacements of these features are observed for enriched and depleted samples in comparison to controls, leading to slight changes

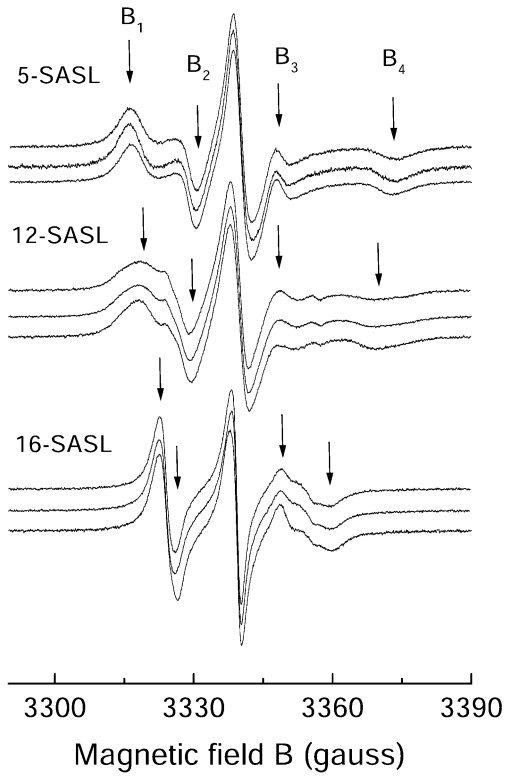


Fig. 1. Electron paramagnetic resonance (EPR) spectra of liposoluble spin labels sensing the lipid bilayer of the erythrocyte membrane at three different levels. Temperature, 25 °C; microwave frequency, 9.75 GHz. Upper group, 5-SASL (labeled moiety at carbon 5, closest to polar headgroups); medium group, 12-SASL (labeled moiety at carbon 12); lower group, 16-SASL (labeled moiety at carbon 16, closest to the bilayer center). For each group of spectra, the central one corresponds to controls (Δ%Chol = 0); upper spectrum corresponds to cholesterol-depleted (Δ%Chol = −33%); and lower spectrum is for cholesterol-enriched erythrocytes (Δ%Chol = 90%). Samples submitted to DPPC liposome treatment. The arrows labeled $B_1$ to $B_4$ point to the spectrum features whose magnetic field positions are used in the calculation of the apparent order parameter $S_{app}$. The spectra of cells treated with MβCD show characteristics similar to those shown in this figure.

in $S_{app}$. A high degree of label immobilization is inferred from the appearance of the spectra of 5- and 12-SASL, indicating a low probability of gauche isomers at the level of carbons 5 and 12 of the acyl chains, both for control and treated samples. In the spectra of 16-SASL, the three narrower lines indicate higher degrees of freedom

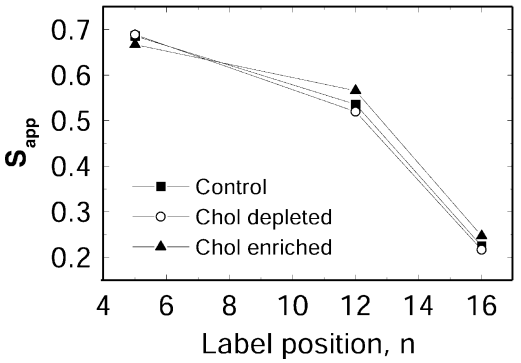


Fig. 2. Apparent order parameters calculated from the EPR spectra shown in Fig. 1, as a function of the position, *n*, of the labeled moiety along the acyl chain. Triangles, cholesterol enriched (Δ%Chol = 90%); circles, cholesterol depleted (Δ%Chol = −33%); squares, control erythrocytes (Δ%Chol = 0). Samples submitted to DPPC liposome treatment. Vertical error bars are smaller than the symbol sizes.

of the nitroxide moiety, with axial restrictions. Similar EPR spectra were obtained for MβCD treated cells.

Apparent order parameters $S_{app}$ were calculated for each experiment and each label, together with the level of significance for the hypothesis of different $S_{app}$ values between controls and treated samples (two-tailed Student's *t*-test, Table 1).

To compare the way in which order parameters are modified along depth in the bilayer, $S_{app}$ values for cells with membranes enriched to 190% and depleted to 67% of their original cholesterol content (samples corresponding to the spectra shown in Fig. 1), were plotted in Fig. 2 as a function of the carbon number where the nitroxide radical is located. Control $S_{app}$ values were also included. It can be seen in Fig. 2 that the slope between carbons 5 and 12 suffers slight changes: it increases in cholesterol depleted samples, and decreases in cholesterol enriched samples, compared to controls. Similar trends were observed in the remaining experiments.

In order to perform a more precise quantification of these effects, the differences in $S_{app}$ between treated and control cells for each label and for each cholesterol concentration were calculated as:

$$\Delta S_{app} = S_{app}^{treated} - S_{app}^{control}$$

$\Delta S_{app}$ values for the three labels, for all the treated samples (either by liposome or MβCD methods) are plotted in Fig. 3 as a function of the percentage variation in membrane cholesterol concentration, defined as:

$$\Delta\%[chol] = 100 \times ([chol]^{treated} - [chol]^{control})/[chol]^{control}$$

A linear regression was performed in order to fit the experimental data of Fig. 3. The correlation coefficients are reported in the figure caption.

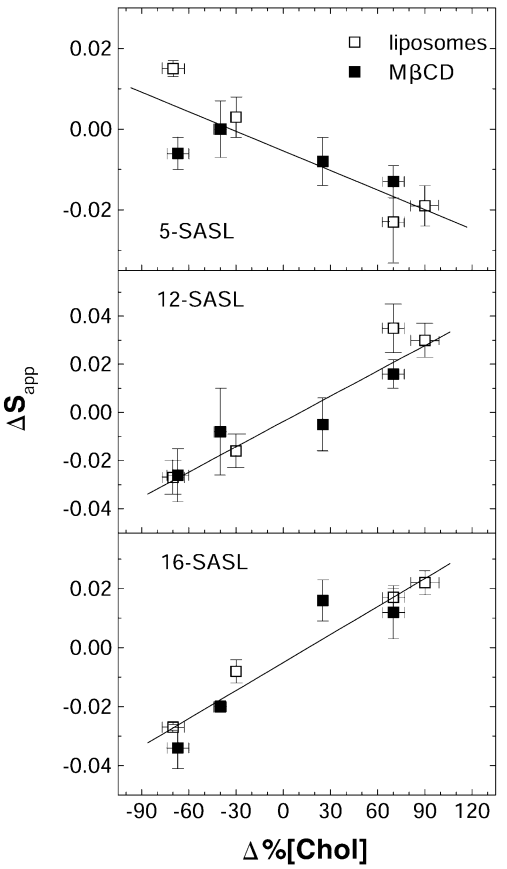


Fig. 3. Differences in EPR apparent order parameter $\Delta S_{app} = S_{app}^{treated} - S_{app}^{control}$ for all the experiments, plotted as a function of percent cholesterol changes in erythrocyte membranes. In each plot, open symbols correspond to liposome-treated erythrocytes, and full symbols correspond to MβCD treated erythrocytes. Solid lines correspond to linear fits. Linear correlation coefficients of these fittings are: 5-SASL, $R = -0.860$; 12-SASL, $R = 0.968$; 16-SASL, $R = 0.987$.

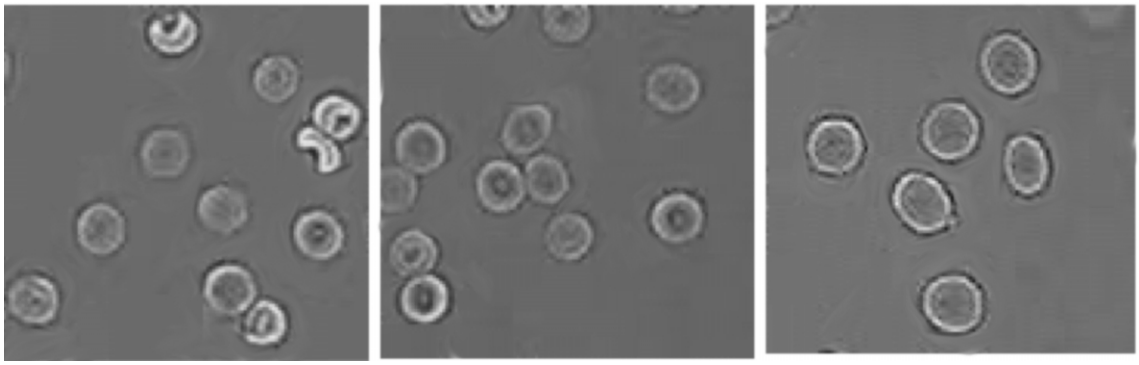

Fig. 4. Unfixed erythrocytes incubated with liposomes (magnification, 400×). Left panel: cholesterol depleted erythrocytes ($\Delta$%Chol = −33%) after 30 h incubation with DPPC liposomes. Central panel: control erythrocytes ($\Delta$%Chol = 0) after 30 h incubation in a medium lacking of liposomes. Right panel: cholesterol enriched erythrocytes ($\Delta$%Chol = +90%) after 30 h incubation with DPPC/cholesterol liposomes. Photographs were taken by digital video imaging.

Their absolute values are very near to 1, indicating that the changes in order parameter are strongly correlated to the changes in cholesterol content in the membranes. It is interesting to remark the inverse behavior observed for the order parameter sensed by 5-SASL in comparison with those sensed by 12- and 16-SASL. Increases in cholesterol concentration ($\Delta$%[chol] > 0) increase the order parameter ($\Delta S_{app} > 0$) at the level of carbons $12^{th}$ and $16^{th}$ (12- and 16-SASL), but decrease $S_{app}$($\Delta S_{app} < 0$) near the polar heads (5-SASL). For cholesterol depleted samples, the behavior is exactly opposite.

It is observed that MβCD treated cells have higher dispersions from the regular behavior when compared to liposome treated samples.

### *3.3. Effects of different treatments on cell shape*

Fig. 4 show microscope photographs of unfixed cells after 30 h incubation with liposomes. The central panel shows control erythrocytes; the left panel shows cholesterol depleted erythrocytes by 30 h incubation with dipalmitoyl phosphatidylcholine (DPPC) liposomes, and the right panel shows cholesterol enriched erythrocytes after incubation with DPPC/cholesterol liposomes. It can be assessed in Fig. 4 that cholesterol depleted cells are mainly stomatocytes (left). A significant portion of stomatocytes is also observed among control cells, due to the prolonged incubation in plasma free suspension medium. On the other side, despite the poor definition, the right image shows cholesterol enriched cells that seem to have preserved the discocytic shape. In the case of liposome treatments using dimyristoyl phosphatidylcholine (DMPC), enriched cells showed spiculated shapes (data not shown), which is consistent with the incorporation of small amounts of liposomal DMPC to the erythrocyte membrane. The incorporation of shorter chain phospholipids to the erythrocyte membrane has been studied in detail [31–33], and it was shown that important shape changes like those described by us can be induced by incorporation of only 3% of exogenous phospholipid to the external leaflet of the bilayer. We did not observe these shape modifications in DMPC cholesterol depleted cells, probably due to the compensating effect of cholesterol loss. It should be remarked that even in the case of spiculated shapes, the order parameter sensed by our EPR experiments correlated well with cholesterol content.

Fig. 5 shows microscope photographs of unfixed cells after MβCD treatments. Again, depleted cells have mainly stomatocytic shapes, consistent with the reduction of surface area of the external leaflet of the bilayer resulting from a loss of cholesterol, while enriched cells show preservation of the

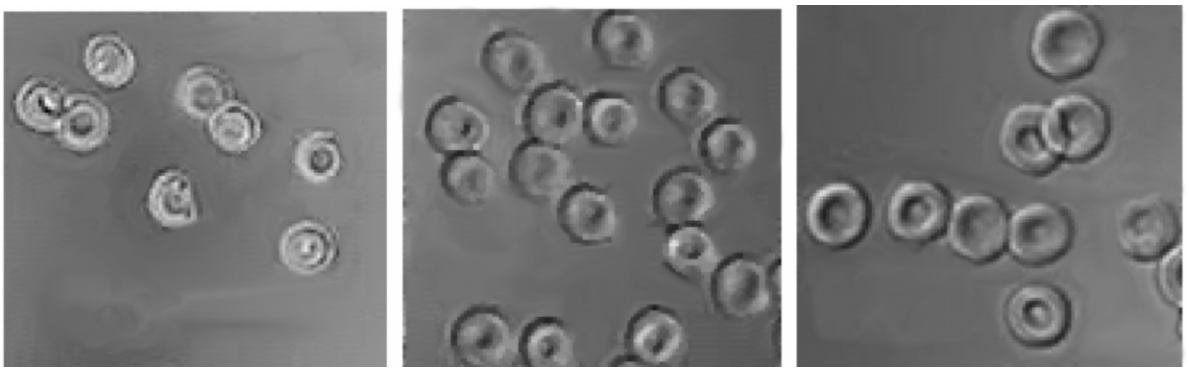

Fig. 5. Unfixed erythrocytes incubated with methyl-β-cyclodextrin (MβCD). (magnification, 400×). Left panel, cholesterol depleted erythrocytes (Δ%Chol = −67%) after 30 min incubation in 3 mM MβCD solution. Central panel, control erythrocytes (Δ%Chol = 0) after 30 min incubation in PBS. Right panel, cholesterol enriched erythrocytes (Δ%Chol = +70%) after 30 min incubation in 3 mM MβCD/cholesterol solution. Photographs were taken by digital video imaging.

original discoid shape, with a slight increase in cell diameter.

Although their definition is poor, these photographs suggest that shape changes after treatments are those expected for the case in which no important variations in lipid content other than cholesterol occur; in the worst case, no more than 5% of foreign DMPC is expected to be incorporated to the external membrane leaflet.

## 4. Discussion

The phenomenon of lateral segregation of lipids in biological membranes, leading to domain formation, is strongly related to acyl chain ordering [8,34,35]. Thus, methods capable of giving detailed information about in-depth variations of chain ordering are of direct relevance to this aspect of membrane biology.

Our goal in the present work has been to detect the response of acyl chain ordering in the erythrocyte membrane upon changes in membrane cholesterol content. This goal was achieved by performing cholesterol enrichment and depletion by two different methods, subsequently introducing lipid-like spin labels, and studying the samples with EPR spectroscopy. In this way, a 'depth profiling' of apparent order parameters was obtained (flexibility gradient, Fig. 2). The negative slope of this depth profiling is due to the accumulation of trans-gauche isomerizations, which cause a decrease in order towards the end of the acyl chains, both for control and treated erythrocytes. Slight variations in slope among control and treated samples are observed in Fig. 2 between the 5$^{th}$ and 12$^{th}$ chain positions, suggesting that the influence of the almost planar cholesterol ring structure in restricting t-g isomerizations of neighbor acyl chains is located at this zone. These results are consistent with previous data about the in-depth cholesterol location in the bilayer [5,35,36]. The variations in order parameter for 16-SASL (increasing in cholesterol enriched, and decreasing in cholesterol depleted cells) likely reflect the accumulation of the effects produced in the upper regions of the corresponding acyl chains.

A high correlation between the measured changes in EPR apparent order parameter and the percentage of changes in cholesterol concentration in the erythrocyte membrane was observed. A positive correlation between $\Delta S_{app}$ and Δ%Chol was obtained for spin labels located at the positions 12 and 16, while $\Delta S_{app}$ sensed by the spin label at position 5 behaves in the opposite way. This means that when cholesterol is increased, acyl chain order is also increased when sensed at position 12 or deeper, but polar headgroup order is decreased, as sensed by 5-SASL. The opposite behavior is observed upon cholesterol depletion. These facts are consistent with results obtained in model sys-

tems by other authors. Marsh [36] determined polarity profiles using spin label EPR in several model membranes in the fluid state, and his results are consistent with the well-known ordering effect of cholesterol on fluid acyl chains, plus a spacing function at the polar headgroup region. Subsczynski et al. [37] observed similar effects of cholesterol on the polarity profiles in frozen membranes. These results coincide with those of a $^{31}P$ NMR study [38], which showed that cholesterol incorporation to synthetic mixtures of membrane lipids disrupts polar headgroup interactions by increasing the separation among them. Also, in a fluorescence study, Ho et al. [39] have shown that acyl chain and headgroup regions are structurally uncoupled.

It is likely that the cholesterol effects reported here are similar to those stabilizing the cholesterol-rich in-plane detergent-insoluble membrane domains (rafts). The existence of erythrocyte rafts has been recently demonstrated, and it has also been reported that these rafts are disrupted after membrane cholesterol depletion [13]. In the context of our results, the increased acyl chain disorder caused by cholesterol depletion would weaken the interactions responsible of the liquid ordered state characteristic of lipid rafts, thus facilitating the detergent solubilization of these otherwise insoluble patches.

In summary, our results show that the increase in cholesterol in erythrocyte membranes stiffens acyl chains but decreases the interaction among lipid headgroups. On the other side, the reduction of cholesterol causes stronger interactions at the headgroup level but disorders the hydrophobic interior. The influence of cholesterol on acyl chain ordering is consistent with results obtained in model systems [5,36–39], but the evidence of an opposite effect on headgroups in a real biomembrane seems to be a novel result of our work.

## Acknowledgments

This work was supported by Universidad Nacional del Litoral (Grant CAI+D 53/96) and by Consejo Nacional de Investigaciones Científicas y Tecnológicas (CONICET, Grant PIP 4807), Argentina. We thank Dr. A. J. Marcipar for allowing us to use laboratory facilities, Prof. V. Mantovani for helpful advice, and Dr Henning Ulrich for critical reading of the manuscript. AMG is a member of CONICET, Argentina.

## References

[1] R.A. Cooper, M.H. Leslie, S. Fischkoff, M. Shinitzky, S.J. Shattil, Factors influencing the lipid composition and fluidity of red cells possessing more than two cholesterols per phospholipid, Biochemistry 17 (1978) 327–331.

[2] H.R. Shmeeda, E.B. Golden, Y. Barenholz, Membrane lipids and aging, in: M. Shinitzky (Ed.), Biomembranes—Structural and Functional Aspects, VCH, Weinheim, 1994.

[3] B.W. van der Meer, Fluidity, dynamics and order, in: M. Shinitzky (Ed.), Biomembranes—Physical Aspects, VCH, Weinheim, 1993.

[4] J.H. Ipsen, G. Karlstrom, O.G. Mouritsen, H. Wennerstrom, M.J. Zuckermann, Phase equilibria in the phosphatidylcholine-cholesterol system, Biochim. Biophys. Acta 905 (1987) 162–172.

[5] T.P.W. McMullen, R.N. McElhaney, Physical studies of cholesterol-phospholipid interactions, Curr. Opin. Colloid Interface Sci. 1 (1996) 83–90.

[6] K. Jacobson, E.D. Sheets, R. Simson, Revisiting the fluid mosaic model of membranes, Science 268 (1995) 1441–1442.

[7] K. Simons, E. Ikonen, Functional rafts in cell membranes, Nature 387 (1997) 569–572.

[8] D.A. Brown, E. London, Structure and origin of ordered lipid domains in biological membranes, J. Membr. Biol. 164 (1998) 103–114.

[9] C. Dietrich, L.A. Bagatolli, Z.N. Volvyk, et al., Lipid rafts reconstituted in model membranes, Biophys. J. 80 (2001) 1417–1428.

[10] G. Civenni, S.T. Test, U. Brodebck, P. Butikofer, In vitro incorporation of GPI-anchored proteins into human erythrocytes and their fate in the membrane, Blood 91 (1998) 1784–1792.

[11] U. Salzer, R. Prohaska, Stomatin, flotillin-1 and flotillin-2 are major integral proteins of erythrocyte rafts, Blood 97 (2001) 1141–1143.

[12] M. Ge, K.A. Field, R. Aneja, D. Holowka, B. Baird, J.H. Freed, Electron spin resonance characterization of liquid ordered phase of detergent-resistant membranes from RBL-2H3 cells, Biophys. J. 77 (1999) 925–933.

[13] B.U. Samuel, N. Mohandas, T. Harrison, et al., The role of cholesterol and glycosylphosphatidylinositol-anchored proteins of erythrocyte rafts in regulating raft protein content and malarial infection, J. Biol. Chem. 276 (2001) 29319–29329.

[14] K. Schorn, D. Marsh, Lipid chain dynamics and molecular location of diacylglycerol in hydrated binary mixtures with phosphatidylcholine: spin label ESR studies, Biochemistry 35 (1996) 831–3836.

[15] M.M. Pincelli, P.R. Levstein, G.D. Fidelio, A.M. Gennaro, Cholesterol induced alterations in the packing properties of gangliosides: an EPR study, Chem. Phys. Lipids 104 (2000) 193–206.
[16] J. Vanderkooi, S. Fischkoff, B. Chance, R. Cooper, Fluorescent probe analysis of the lipid architecture of natural and experimental cholesterol-rich membranes, Biochemistry 13 (1974) 1589–1595.
[17] Y. Lange, J. D'Alessandro, Characterization of mechanisms for transfer of cholesterol between human erythrocytes and plasma, Biochemistry 16 (1977) 4339–4343.
[18] Y. Lange, A.L. Molinaro, T.R. Chauncey, T.L. Steck, On the mechanism of transfer of cholesterol between human erythrocytes and plasma, J. Biol. Chem. 258 (1983) 6920–6926.
[19] R.A. Cooper, Influence of increased membrane cholesterol on membrane fluidity and cell function in human red blood cells, J. Supramol. Struct. 8 (1978) 413–430.
[20] N.L. Thompson, D. Axelrod, Reduced lateral mobility of a fluorescent probe in cholesterol-depleted erythrocyte membrane, Biochim. Biophys. Acta 597 (1980) 155–165.
[21] Y. Ohtani, T. Irie, K. Uekama, K. Fukunaga, J. Pitha, Differential effects of α-, β- and γ-cyclodextrins on human erythrocytes, Eur. J. Biochem. 186 (1989) 17–22.
[22] J. Kavecansky, C.H. Joiner, F. Schroeder, Erythrocyte membrane lateral sterol domains: A dehydroergosterol fluorescence polarization study, Biochemistry 33 (1994) 2880–2890.
[23] P.G. Yancey, W.V. Rodrigueza, E.P.C. Kilsdonk, et al., Cellular cholesterol efflux mediated by cyclodextrins, J. Biol. Chem. 271 (1996) 16026–16034.
[24] A.E. Christian, M.P. Haynes, M.C. Phillips, G.H. Rothblat, Use of cyclodextrins for manipulating cellular cholesterol content, J. Lipid Res. 38 (1997) 2264–2272.
[25] G. Gimpl, K. Burger, F. Fahrenholz, Cholesterol as modulator of receptor function, Biochemistry 36 (1997) 10959–10974.
[26] S. Härtel, H.A. Diehl, F.S. Ojeda, Methyl-β-cyclodextrins and liposomes as water-soluble carriers for cholesterol incorporation into membranes and its evaluation by a microenzymatic fluorescence assay and membrane fluidity-sensitive dyes, Anal. Biochem. 258 (1998) 277–284.
[27] H.G. Rose, M. Oklander, Improved procedure for the extraction of lipids from human erythrocytes, J. Lipid Res. 6 (1965) 428–431.
[28] M.A. Brito, M.R. Silva, D.C. Matos, A.T. da Silva, D.T. Brites, Alterations of erythrocyte morphology and lipid composition by hyperbilirubinemia, Clin. Chimica Acta 249 (1996) 149–165.
[29] H.A. Ahmed, Measurement of cholesterol in membranes, in: J.M. Graham, J.A. Higgins (Eds.), Methods in Molecular Biology, 19, Humana Press Inc, Totowa, NJ, 1993.
[30] O.H. Griffith, P.C. Jost, Spin labels in biological membranes, in: L.J. Berliner (Ed.), Spin Labeling: Theory and Applications, Academic Press, New York, 1976, pp. 454–523.
[31] J.E. Ferrell, K.J. Lee, W.H. Huestis, Membrane bilayer balance and erythrocyte shape: a quantitative assessment, Biochemistry 24 (1985) 2849–2857.
[32] J.E. Ferrell, K.J. Lee, W.H. Huestis, Lipid transfer between phosphatidylcholine vesicles and human erythrocytes: exponential decrease in rate with increasing acyl chain length, Biochemistry 24 (1985) 2857–2864.
[33] D.J. Moore, R.H. Sills, R. Mendelsohn, Conformational order of specific phospholipids in human erythrocytes: correlations with changes in cell shape, Biochemistry 36 (1997) 660–664.
[34] R.E. Brown, Sphingolipid organization in biomembranes: what physical studies of model membranes reveal, J. Cell Sci. 111 (1998) 1–9.
[35] J.P. Slotte, Sphingomyelin-cholesterol interactions in biological and model membranes, Chem. Phys. Lipids 102 (1999) 13–27.
[36] D. Marsh, Polarity and permeation profiles in lipid membranes, Proc. Natl. Acad. Sci. USA 98 (2001) 7777–7782.
[37] W.K. Subczynski, A. Wisniewska, J.J. Yin, J.S. Hyde, A. Kusumi, Hydrophobic barriers on lipid bilayer membranes formed by reduction of water penetration by alkyl chain unsaturation and cholesterol, Biochemistry 33 (1994) 7670–7681.
[38] P.L. Yeagle, W.C. Hutton, C. Huang, R. Bruce Martin, Phospholipid head-group conformations; intermolecular interactions and cholesterol effects, Biochemistry 16 (1977) 4344–4349.
[39] C. Ho, S.J. Slater, C.D. Stubbs, Hydration and order in lipid bilayers, Biochemistry 34 (1995) 6188–6195.